lyophilization from 99.8% $D_2O$. Proton NMR spectra were recorded on a Bruker WM-300 spectrometer. Suppression of the residual HDO peak was achieved by a low-power selective irradiation pulse (during 0.8 s).

The assignments of the resonances in the spectra (Tables III and IV) to individual protons are based on the following rationales: The $H_1$ ($OCH_3$) resonance is readily recognized as a singlet at 3.4 ppm. Vicinally coupled pairs of protons were identified by extensive decoupling experiments. The stereochemical assignment of the geminal $H_{2'}$ and $H_{2''}$ is based on coupling constant considerations. The assignments of the $H_{5'}$ and $H_{5''}$ signals conform to the assignment reported previously for tetrahydrofuranmethanol.[10] The resolution-enhanced 300-MHz spectra were computer simulated with a LAOCOON-type computer program of which the standard plot routines were extended[38] in order to reproduce Gaussian line shapes with negative side lobes.

Pseudorotational phase angles ($P$), puckering amplitudes ($\Phi_m$), and mole fractions of conformers ($X_N$, $X_S$) were calculated from the experimental vicinal coupling constants with the computer program PSEUROT. This program is based on algorithms as described by Haasnoot et al.[8] and De Leeuw et al.[39,40]

**Acknowledgment.** This research was supported by The Netherlands Foundation for Chemical Research (SON) with financial aid from The Netherlands Organization for the Advancement of Pure Research (ZWO). We gratefully acknowledge the stimulating discussions with Prof. Dr. C. W. Hilbers and Prof. Dr. C. Altona.

(38) Mellema, J.-R.; Pieters, J. M. L.; van der Marel, G. A.; van Boom, J. H.; Haasnoot, C. A. G.; Altona, C. *Eur. J. Biochem.* **1984**, *143*, 285.

(39) de Leeuw, F. A. A. M.; Altona, C. *J. Comput. Chem.* **1983**, *4*, 438.
(40) de Leeuw, F. A. A. M.; Altona, C. *QCPE* **1983**, *463*.

# Aqueous Coordination and Location of Exchangeable $Cu^{2+}$ Cations in Montmorillonite Clay Studied by Electron Spin Resonance and Electron Spin–Echo Modulation

**David R. Brown[†] and Larry Kevan***

*Contribution from the Department of Chemistry, University of Houston, Houston, Texas 77004.*
*Received June 23, 1987*

**Abstract:** Electron spin resonance (ESR) and electron spin–echo modulation (ESEM) spectroscopies have been used to characterize the aqueous coordination and location of exchangeable $Cu^{2+}$ cations in the interlayer regions of montmorillonite clay. $Mg^{2+}$ montmorillonite, in which 5% of the exchangeable cations were replaced by $Cu^{2+}$, was investigated. Under complete hydration, ESR indicates freely rotating $Cu^{2+}$ ions in the interlayer region, and the corresponding ESEM indicates six directly bound water molecules. Under partial dehydration ESR shows $Cu^{2+}$ in a second site with restricted rotation, and the corresponding ESEM indicates coordination to four water molecules. Following the collapse of the aqueous interlayer region on further dehydration, the $Cu^{2+}$ enters a third site in a hexagonal cavity of the lattice structure, also with restricted rotation, in which it remains coordinated to only one water molecule. The natures and interconversions of these three sites are discussed.

The two swelling phyllosilicates, montmorillonite and hectorite, are members of the smectite group of clays. These clays have a layered structure in which rigid layers of silicate ions are separated by aqueous interlayer regions containing hydrated cations as shown in Figure 1. The thickness of the aqueous interlayer region is sensitive to ambient conditions and can readily be varied from many molecular layers to almost zero by controlled hydration and dehydration. The location and solvation of the cations in this interlayer region depend on several factors, including the thickness of the aqueous interlayer, the location and abundance of anionic sites in the clay lattice, and the presence of cavities in the clay lattice which can accomodate and chelate the cations.

The anionic lattice sites in montmorillonite and hectorite are in the middle, octahedral, layer of the smectite structure, and as such they are separated from the cations by the upper and lower tetrahedral layers. The relatively weak electrostatic attraction between cations and anionic sites means that, under appropriate conditions, the cations can move away from the silicate surface into the body of a strongly solvating solvent, where strong solvation compensates for the increased electrostatic potential energy. On removal of the solvent by dehydration cations are thought to enter hexagonal cavities in the silicate lattice.[1] These have internal diameters of about 0.5 nm and can accomodate all but the largest cations. Once in these cavities cations are coordinated by lattice oxygens.

Several techniques have been used to study cation locations in clays. X-ray diffraction has been of limited use because of the poor crystallinity typically exhibited by clays. Among other spectroscopic techniques electron spin resonance (ESR) has been one of the most successful, even though its use is limited to clays containing paramagnetic centers.[2-5]

An ESR study of a magnesium hectorite, in which 5% of the exchangeable cations were replaced with $Cu^{2+}$, revealed two discrete $Cu^{2+}$ centers, one dominating in fully hydrated clay and a second in clay that has been equilibrated at room temperature and 40% relative humidity.[3] The appearance of these two species was correlated with different $d_{001}$ basal spacings determined from X-ray powder diffraction. The first $Cu^{2+}$ center was assigned to a fully hydrated, freely rotating $Cu^{2+}$ in an aqueous layer of several water molecular thicknesses. The second $Cu^{2+}$ center was associated with a water interlayer of thickness 0.5 nm, and was assigned to a rotationally restricted $[Cu(H_2O)_6]^{2+}$ solvate. However, the aqueous coordination numbers have only been inferred and have not been directly determined.

[†] Present address: Department of Applied Science, Leeds Polytechnic, Leeds, LS1 3HE, England.

(1) Grim, R. E. *Clay Mineralogy*, 2nd ed.; McGraw-Hill: New York, 1968.
(2) Pinnavaia, T. J. In *Advanced Techniques for Clay Mineral Analysis*; Fripiat, J. J., Ed.; Elsevier: New York, 1981; p 139.
(3) McBride, M. B.; Pinnavaia, T. J.; Mortland, M. M. *J. Phys. Chem.* **1975**, *79*, 2430.
(4) Clementz, D. M.; Pinnavaia, T. J.; Mortland, M. M. *J. Phys. Chem.* **1973**, *77*, 196.
(5) McBride, M. B. *Clays Clay Miner.* **1982**, *30*, 200.

0002-7863/88/1510-2743$01.50/0 

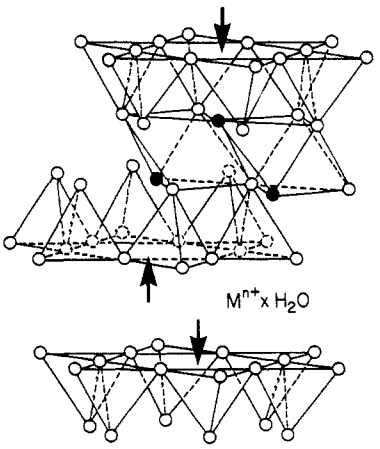


**Figure 1.** Schematic representation of the oxygen network in smectite clays where open circles are oxygen and dark circles are OH. The hydrated interlayer exchangeable cations are represented, but nonexchangeable cations within the octahedral and tetrahedral sites of the silicate sheets have been omitted for clarity. Arrows identify the hexagonal cavities in the upper and lower silicate sheets.

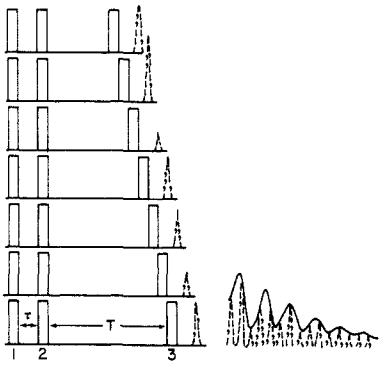


**Figure 2.** Illustrations of modulation of a three-pulse spin–echo decay envelope. The time $\tau$ between microwave pulses 1 and 2 is kept fixed while the time $T$ between pulses 2 and 3 is varied. The echo appears at time $\tau$ after pulse 3. As $T$ is increased the amplitude varies as shown from top to bottom and traces out a modulated echo intensity as shown.

The ESR spectrum of $Cu^{2+}$ in a fully dehydrated smectite has not been reported. However, the spectrum of $Mn^{2+}$, doped into the same magnesium hectorite, has been measured on complete dehydration, and interpreted in terms of $Mn^{2+}$ ions entering the hexagonal cavities.[3] Whether the cation remains solvated to any extent after entering the cavity is unknown.

The objective of this study is to use ESR and three-pulse electron spin–echo modulation (ESEM) spectroscopy to directly determine the aqueous coordination of exchangeable $Cu^{2+}$ in smectite clays under the various conditions of hydration. The theory and analysis of ESEM have been described.[6-8] A three-pulse sequence was used as shown in Figure 2 to generate an echo at time $\tau$ (see Figure 2) after the third pulse. The echo amplitude as a function of interpulse time $T$ is modulated by weak dipolar electron-nuclear hyperfine interaction with neighboring magnetic nuclei. The resulting modulation pattern is simulated as a function of the number of approximately equivalent nearest nuclei coupled to the paramagnetic ion, their distance from the ion, and the isotropic hyperfine coupling constant.[7] Determination of the number of coupled nuclei in solvent water molecules together with their distance from $Cu^{2+}$ gives a direct measurement of the aqueous coordination number. Deuterium modulation gives deeper modulation than protium modulation and can be analyzed more quantitatively so the clay systems were exchanged with $D_2O$.

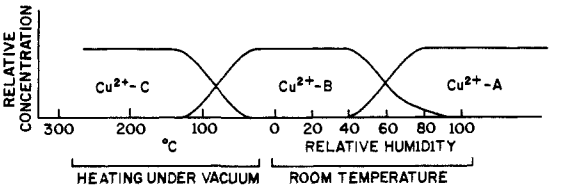


**Figure 3.** The dependence of the relative concentrations of $Cu^{2+}$ species, A, B, and C in $Mg^{2+}$ montmorillonite (5% $Cu^{2+}$) on hydration/dehydration conditions. The relative concentrations have been assessed from the relative intensities of the corresponding ESR signals recorded at 77 K.

Protium modulation was suppressed by using lower amplitude pulses that do not excite protium modulation.[6] Three-pulse ESEM is advantageous for solvation studies on surfaces containing a magnetic nucleus such as $^{27}Al$ because interpulse time $\tau$ (see Figure 2) can be chosen to suppress modulation from one type of nucleus without interfering with that from another. The usefulness of ESEM in this study lies in its ability to detect very weak hyperfine interactions, interactions that are undetectable with continuous wave ESR in powder systems.

## Experimental Section

A natural montmorillonite clay, STx-1, supplied by the Clay Resource Repository, University of Missouri, was used for this work. This mineral has been fully characterized[9] and has a cation exchange capacity of 84.4 meq/100 g, with $Ca^{2+}$ as the major cation.

The clay was washed briefly with 0.05 M HCl solution to remove calcium carbonate. It was then sitrred in 1.5 M $MgCl_2$ solution for 24 h, washed, and treated with $MgCl_2$ solution again to ensure complete exchange of $Mg^{2+}$ for $Ca^{2+}$. The clay was then washed several times with water, using a centrifuge to separate washings, until the supernatant formed no AgCl precipitate with $AgNO_3$ solution. The clay was then stirred for 24 h with an appropriate concentration of $CuCl_2$ solution to exchange $Cu^{2+}$ for 5% of the cation sites. The clay was again washed until the supernatant was free of $Cl^-$, and allowed to dry at room temperature.

A similar procedure was used to prepare fully exchanged $Cu^{2+}$ montmorillonite. The $Ca^{2+}$ montmorillonite was stirred for 24 h in an excess of 1.5 M $CuCl_2$ solution. After washing, the process was repeated to ensure complete exchange. Commercial microanalyses were performed on all samples for Ca, Mg, and Cu.

Samples of powdered clay were equilibrated at several relative humidities from 0 to 100% at room temperature. Controlled relative humidities were established in sealed vessels using suitable $H_2O/H_2SO_4$ mixtures. In addition, samples of clay were evacuated to $1 \times 10^{-6}$ torr for several hours at room temperature and at elevated temperatures to 300 °C.

X-ray basal spacings were measured on a Philips diffractometer with a vertical goniometer, using the copper $K_\alpha$ line. Infrared data were collected on a Perkin-Elmer 330 spectrophotometer fitted with an integrating sphere accessory to obtain reflectance measurements using $BaSO_4$ as a reflectance standard. ESR spectra were recorded on an IBM SP200 spectrometer at 77 and 300 K. ESE spectra were recorded at 4 K on a home-built spectrometer described elsewhere.[10-12] Three-pulse stimulated echoes were recorded to observe modulation from both D ($\tau$ = 0.27 $\mu$s) and $^{27}Al$ ($\tau$ = 0.4 $\mu$s).

Several methods of exchanging $D_2O$ for $H_2O$ were tried. The degree of exchange was measured from the infrared diffuse reflectance spectra and by monitoring the depth of modulation in the ESEM pattern. Essentially complete exchange was accomplished by evacuating the clay for 24 h to $10^{-6}$ torr, followed by distillation of excess $D_2O$ onto the clay, which was allowed to soak for a further 24 h. The procedure was repeated twice with each sample. $D_2O$ (99.5%) was supplied by the Aldrich Chemical Co.

Oriented films of clay were prepared by allowing suspensions of the clay to dry on thin glass plates. Sections of the plates holding the films were inserted into ESR tubes and subjected to the same thermal/vacuum treatments as the powders. The ESR spectra of the films were recorded at specific angles with respect to the magnetic field. It was not possible

(6) Kevan, L. In *Time Domain Electron Spin Resonance*; Kevan, L., Schwartz, R. N., Eds.; Wiley-Interscience: New York, 1979; Chapter 8.
(7) Ichikawa, T.; Kevan, L.; Bowman, M. K.; Dikanov, S. A.; Tsvetkov, Y. D. *J. Chem. Phys.* **1979**, *71*, 1167.
(8) Kevan, L. *J. Phys. Chem.* **1981**, *85*, 1628.
(9) *Data Handbook for Clay Minerals and Other Non Metallic Minerals*; Van Olphen, M., Fripiat, J. J., Eds.; Pergamon: Oxford, 1979; p 22.
(10) Ichikawa, T.; Kevan, L.; Narayana, P. A. *J. Phys. Chem.* **1979**, *83*, 3378.
(11) Narayana, P. A.; Kevan, L. *Magn. Reson. Rev.* **1983**, *1*, 234.
(12) Narayana, P. A.; Kevan, L. *Photochem. Photobiol.* **1983**, *37*, 105.

**Table I.** ESR Parameters and X-ray Diffraction Spacing ($d_{001}$) for $Cu^{2+}$ Exchanged Smectites

| | $d_{001}$ (nm) | $T$ (K) | $g_{\parallel}$ | $A_{\parallel}$[a] | $g_{\perp}$ |
|---|---|---|---|---|---|
| $Cu^{2+}$ montmorillonite | | | | | |
| hydrated at 100% RH | 2.0 | 77 | 2.39 | 145 | 2.09 |
| | | 300 | $g_{iso}$ = 2.17 | | |
| dried at 0% RH | 1.2 | 77 | 2.38 | 172 | 2.08 |
| evacuated at 150 °C | 1.0 | 77 | 2.42 | 115 | 2.09 |
| $Cu^{2+}$ hectorite[b] | | | | | |
| air-dried | 1.24 | 77 | 2.33 | 175 | 2.08 |
| | | 300 | 2.34 | 165 | 2.08 |
| $Cu^{2+}$ montmorillonite[b] | | | | | |
| air-dried | monolayer of water | 77 | 2.34 | 175 | 2.09 |
| $Mg^2$ montmorillonite (5% $Cu^{2+}$) | | | | | |
| hydrated at 100% RH | 2.0 | 77 | 2.41[c] | 142 | 2.09 |
| | 2.0 | 300 | $g_{iso}$ = 2.18 | | |
| dried at 0% RH | 1.2-1.7 | 77 | 2.35[d] | 178[e] | 2.07 |
| | 1.2-1.7 | 300 | 2.35 | 175[e] | 2.07 |
| evacuated at 150° C | 1.0 | 77 | 2.42[f] | 117 | 2.09 |
| | 1.0 | 300 | 2.42 | 117 | 2.09 |
| $Mg^{2+}$ hectorite[g] (5% $Cu^{2+}$) | | | | | |
| air-dried | 1.47 | 298 | 2.335 | 156[h] | 2.065 |

[a] Units of $10^{-4}$ $cm^{-1}$. [b] Reference 4. [c] $Cu^{2+}$ species A. [d] $Cu^{2+}$ species B. [e] $A_{\perp}$ = 30 × $10^{-4}$ $cm^{-1}$. [f] $Cu^{2+}$ species C. [g] Reference 3. [h] $A_{\perp}$ = 22 × $10^{-4}$ $cm^{-1}$.

to record ESE spectra of oriented films because of low signal levels.

## Results

ESR spectra were recorded of $Mg^{2+}$ montmorillonite (5% $Cu^{2+}$) that had been equilibrated at various relative humidities at room temperature, and samples that had been evacuated at room temperature and above. Three distinct $Cu^{2+}$ centers were detected, and conditions were identified that would lead to the formation of each one of these species in the absence of the other two. The semiquantitative diagram in Figure 3 is based on ESR intensities of 10–20% relative accuracy of the various $Cu^{2+}$ species and illustrates the effect of ambient conditions on the $Cu^{2+}$ type. The ESR parameters of these species are listed in Table I. X-ray $d_{001}$ basal spacings corresponding to the conditions for formation are also recorded. Subtracting 0.96 nm, the thickness of the silicate layer, from these values gives the thickness of the aqueous interlayer.

**$Cu^{2+}$ Species A.** $Cu^{2+}$ species A is the dominant $Cu^{2+}$ center at high humidity and in fully wetted clay. Its ESR spectrum at room temperature is given in Figure 4 and is isotropic, suggesting a freely tumbling $Cu^{2+}$ ion. The basal spacing of 2.0 nm corresponds to several layers of water.

Species A gives a very strong spin echo. The ESEM decay is shown in Figure 4c. It is characterized by very deep modulation at short $T$ values which rapidly diminishes as $T$ increases. This is typical of short-range interaction with deuterium nuclei and is due to coupling between $Cu^{2+}$ and deuterium nuclei in the first $D_2O$ solvation shell. The simulated decay envelope represents the best fit achievable by varying the parameters $n$ (number of coupled D nuclei), $r$ (D to $Cu^{2+}$ distance), and $a_{iso}$ (isotropic component of the hyperfine interaction). The $n$ and $r$ parameters are the most critical and informative. In assessing the best fit, more weight has been given to short $T$ values since it is in this region that the modulation pattern is most sensitive to changes in the parameters $n$ and $r$. The best fit corresponds to 12 (±1) deuterium nuclei at a distance of 0.29 (±0.01) nm.

**$Cu^{2+}$ Species B.** Partial dehydration of the clay produces $Cu^{2+}$ species B. It was found that drying at 0–40% relative humidity produces species B exclusively.

The 001 reflection in the X-ray diffraction pattern, on which basal spacing calculations were based, was rather broad in samples exhibiting species B spectra. Although a mean basal spacing of 1.5 nm was calculated, it is possible that the breadth indicates a range of basal spacings from about 1.2 nm to about 1.7 nm.

The ESR and ESEM data of $Cu^{2+}$ species B are shown in Figure 5. The ESR of oriented films of $Mg^{2+}$ montmorillonite

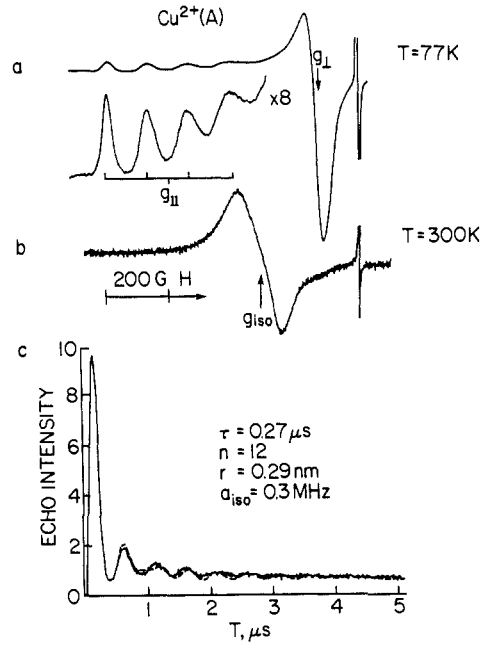


**Figure 4.** The ESR spectra and ESEM pattern of $Cu^{2+}$ species A in $Mg^{2+}$ montmorillonite (5% $Cu^{2+}$), following 24 h at 100% relative humidity. (a) ESR spectrum recorded at 77 K. The intense peak at high field is a DPPH marker. (b) ESR spectrum recorded at 300 is K. (c) Experimental (—) and simulated (---) three-pulse ESE modulation spectrum recorded at 4 K.

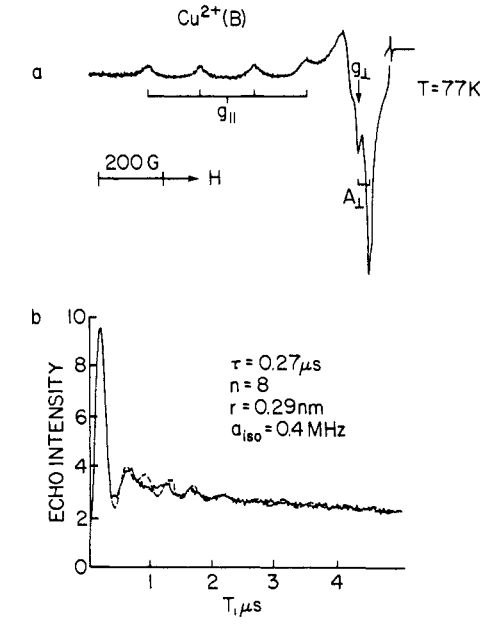


**Figure 5.** (a) ESR spectrum of $Cu^{2+}$ species B in $Mg^{2+}$ montmorillonite (5% $Cu^{2+}$) at 77 K, following 24 h at 0% relative humidity. Hyperfine structure due to coupling with the Cu nucleus is clearly resolved in the parallel region and partially resolved in the perpendicular region shown as $A_{\perp}$. (b) Experimental (—) and simulated (---) three-pulse ESE modulation spectrum of the same sample, recorded at 4 K.

(5% Cu), shown in Figure 6, demonstrates that the axially symmetric $Cu^{2+}$ has its parallel axis at right angles to the clay film, and hence the clay layers, and its perpendicular axis in the plane of the film, consistent with previous results.[3]

The ESEM pattern is again characteristic of short-range coupling to deuterium nuclei, and a good fit simulation is achieved for coupling to 8 ± 1 deuterium nuclei at 0.29 nm. ESEM spectra, recorded with $\tau$ reset to 0.4 μs, showed no modulation attributable to neighboring $^{27}Al$ nuclei.

**$Cu^{2+}$ Species C.** $Cu^{2+}$ species C is formed on complete dehydration of the clay. It was not possible to obtain reliable X-ray

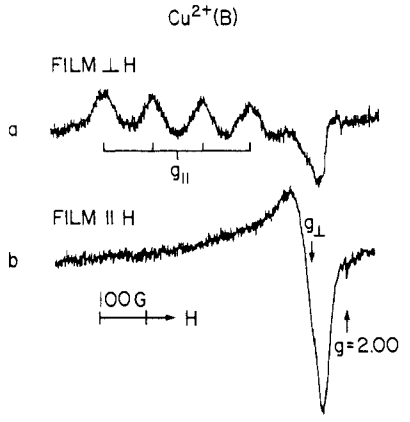


**Figure 6.** ESR spectra of $Cu^{2+}$ species B in $Mg^{2+}$ montmorillonite (5% $Cu^{2+}$) recorded at 300 K on an oriented film of the clay. The spectra was recorded (a) with the magnetic field perpendicular to the plane of the film and (b) with the magnetic field direction parallel to the plane of the film.

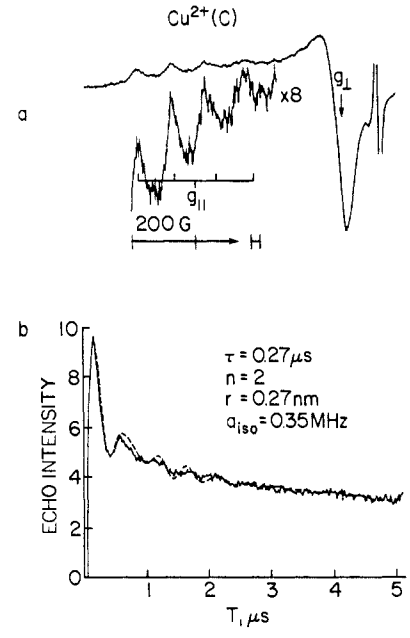


**Figure 7.** (a) ESR spectrum of $Cu^{2+}$ species C in $Mg^{2+}$ montmorillonite (5% $Cu^{2+}$), following dehydration under vacuum at 150 °C (spectrum recorded at 77 K). (b) Experimental (—) and simulated (---) ESE modulation spectrum of $Cu^{2+}$ species C in the same sample, recorded at 4 K.

data on the fully dehydrated clay with the available equipment, but the dehydration behavior of montmorillonite is well documented,[1,5] and under the conditions required to osberve species C no discrete water layers remain in the interlayer region.

The ESR spectrum shows axial symmetry. The ESR spectra of oriented films demonstrate that the parallel axis is at right angles to the plane of the clay, and the perpendicular axes are in the plane, even though the dehydration process evidently causes much of the film to become disoriented.

The ESEM decay associated with species C again shows modulation whose intensity rapidly diminishes as $T$ increases, consistent with closely coupled deuterium nuclei. However, the modulation is quite weak and the best fit simulation corresponds to two deuterium nuclei at 0.27 nm. No modulation attributable to coupling with Al nuclei was found.

It was possible to reverse the conversion of species A to species C by rehydration of the clay, but only if the dehydration temperature had been below 150 °C. If species C had been formed by dehydration at a higher temperature the rehydration failed to reconvert all of species C back to species A. If the dehydration temperature was even higher, 300 °C, then rehydration had no effect on the ESR spectrum and species C remained dominant. X-ray diffraction of these rehydrated clays showed $d_{001}$ spacings of 0.2 nm on rehydration which eliminates the possibility of extensive collapse of the interlayer regions as a cause for this irreversible formation of species C.

**Infrared Measurements.** The efficiency of $D_2O$ exchange for ESEM measurements was examined by near-infrared diffuse reflectance spectra of the clay samples. $H_2O$ was monitored using its band at 1910 nm, and for $D_2O$ the band at 1998 nm was used.[13] Following a twice-repeated exchange process, as described above, replacement of $H_2O$ by $D_2O$ was essentially complete.

The infrared spectrum was also used to monitor the lattice OH groups before and after the exchange process.[13] These are located in the hexagonal cavities and could be involved in coordination should the $Cu^{2+}$ ion enter the cavities. The lattice OH (2206 and 1410 nm) was found to be unaffected by the exchange process and is not converted to OD (1884 nm).

**Fully Exchanged $Cu^{2+}$ Montmorillonite.** Three types of $Cu^{2+}$ center are detected as shown in Table I. The first, found in hydrated $Cu^{2+}$ montmorillonite, is largely similar to species A described above. The second, found in air-dried $Cu^{2+}$ montmorillonite, is similar to species B above, except that the X-ray band spacing associated with its formation is less, as found by previous workers[4] with fully exchanged $Cu^{2+}$ hectorite. In fully dehydrated samples a center similar to species C is detected.

The ESR features are invariably much broader than those for the $Cu^{2+}$-doped $Mg^{2+}$ montmorillonite. Undoubtedly, dipolar broadening in the fully exchanged montmorillonite is responsible. Electron spin–echoes could not be detected for the fully exchanged montmorillonite almost certainly because of the same dipolar interactions.

## Discussion

**$Cu^{2+}$ Species A.** The fully hydrated $Mg^{2+}$ montmorillonite contains several molecular water layers in the interlayer region. The ESR results are indicative of rotationally unrestricted $Cu^{2+}$ on the ESR time scale, presumably free of major influence from the silicate surface. It has been shown, by nuclear magnetic resonance, that the first one or two monolayers of water adjacent to the silicate surfaces exhibit restricted motion,[14] so clearly the $Cu^{2+}$ solvate exists outside this region.

Analysis of the ESEM spectrum indicates 12 approximately equivalently coupled deuterium nuclei corresponding to a water solvation number of six. This is the first direct determination of the solvation number, and it indicates that $[Cu(H_2O)_6]^{2+}$ is the favored structure of species A in an essentially aqueous environment. Thus, in fully hydrated montmorillonite exchangeable cations are fully hydrated.

Hall et al.[15] came to similar conclusions following a quasi-elastic neutron scattering study of $Ca^{2+}$ hydrated montmorillonite, in which they demonstrated that exchangeable $Ca^{2+}$ ions and other exchangeable cations in this environment are freely rotating and fully solvated, although the number of waters was not explicitly determined. ESR studies on fully hydrated $Mn^{2+}$ and $VO_2^+$ ions in the interlayer regions of smectite clays also support this model. The similarity of these solvates to those found in purely aqueous solution was illustrated by their ESR correlation times, which were found to be only 30 to 50% longer in the interlayer environment than for the same ions in dilute aqueous solution.[16-19] However, there are some real differences between cations in water and

(13) Cariati, F.; Erre, L.; Micera, G.; Piu, P.; Gessa, C. *Clays Clay Miner.* **1981**, *29*, 157.
(14) Woessner, D. E. *J. Magn. Reson.* **1980**, *39*, 297.
(15) (a) Hall, P. L.; Ross, D. K. In *Advanced Techniques for Clay Mineral Analysis*; Fripiat, J. J., Ed.; Elsevier: New York, 1981; p 71. (b) Hall, P. L.; Ross, D. K.; Tuck, J. J.; Hayes, M. H. B. *Dev. Sedimentol.* **1979**, *27*, 121.
(16) McBride, M. b.; Pinnavaia, T. J.; Mortland, M. M. *Am. Mineral.* **1975**, *60*, 60.
(17) McBride, M. B. *Clays Clay Miner.* **1979**, *27*, 91.
(18) Raman, K. V.; Mortland, M. M. *Clays Clay Miner.* **1968**, *16*, 393.
(19) Mortland, M. M.; Fripiat, J. J.; Chaussidon, J.; Uytterhovan, J. *J. Phys. Chem.* **1963**, *67*, 248.

cations in the interlayer region of hydrated smectites. It has been shown in several studies that intercalated hydrated cations are more acidic than the same cations in true aqueous environments based on the rates of acid-catalyzed reactions.[18-22] No specific physical explanation of this increased acidity has been substantiated but polarization effects have been suggested to increase the cation acidity for those cations that are closer to a silicate surface.

**$Cu^{2+}$ Species B.** The occurrence of species B is associated with an average basal spacing of 1.5 nm, which corresponds to between two and three layers of water in the interlayer region. However, the breath of the 001 reflectance maximum is also consistent with a range of basal spacings from about 1.2 to about 1.7 nm. This can be understood in terms of an interstratified clay structure with some interlayers containing one molecular layer of water, some two and some three.

Natural smectite clays, such as the montmorillonite studied here, normally exhibit some heterogeneous charge distribution,[1] and it is not surprising that an interstratified structure is formed under these intermediate hydration conditions. It seems reasonable that interlayers of low charge density absorb water relatively easily and therefore show large basal spacings. Similarily, interlayers of high charge density would be expected to exhibit small basal spacings. Clearly, the observation of a single $Cu^{2+}$ species under these conditions suggests that $Cu^{2+}$ ions preferentially occupy only one of these possible types of hydrated interlayer regions.

The number of molecular water layers in the interlayer might be expected to have some influence on the solvation of $Cu^{2+}$ ions present. For instance, a single layer of water would allow solvation by a maximum of four in-plane water molecules, whereas in interlayers of two or three molecular thicknesses of water higher solvation numbers would be possible.

One advantage of the ESEM analysis is that it can count the number of coordinated water molecules, and, for species B, this number is unambigiously less than for fully hydrated $Cu^{2+}$; compare Figures 4c and 5c. Simulation indicates eight coupled deuterium nuclei corresponding to a maximum water solvation number of four.

ESR measurements show that the major axis of symmetry of species B is perpendicular to the plane of the clay structure (Figure 6). The only geometry consistent with both the ESEM and ESR data is square-planar coordination, with the four coordinated water molecules in the same plane as the silicate layer. Such a model is consistent with the shift in $g_{\|}$ toward free spin that is seen on going from species A to species B. This indicates a strengthening of equatorial bonding on going from A to B, which would be anticipated if the conversion of species A to B involved the weakening, and eventual loss, of the two axial ligands. Thus, a solvate of the form $[Cu(H_2O)_4]^{2+}$ is favored, in which all four water molecules are equatorially coordinated.

This model, together with the observation of restricted rotation of the solvate, can only be explained by $Cu^{2+}$ ions preferentially occuping interlayers containing single molecular layers of water. It differs from that proposed by Pinnavaia et al.[3], who studied a similar system, $Mg^{2+}$ hectorite (5% $Cu^{2+}$), and concluded that air drying produced a structure that was not interstratified but did, indeed, exhibit uniform interlayers of between two and three water molecular thickness, in which $Cu^{2+}$ ions existed as rotationally restricted hexahydrates, $[Cu(H_2O)_6]^{2+}$. The unambiguous determination of solvation number from ESEM data, described above, precludes such a model.

It is useful to compare species B formed in $Mg^{2+}$ montmorillonite (5% $Cu^{2+}$) with the similar species formed in fully exchanged $Cu^{2+}$ montmorillonite under the same conditions. The ESR parameters of the two species are very similar. In the fully $Cu^{2+}$ exchanged montmorillonite X-ray diffraction data clearly shows hydration by a single molecular layer of water in the interlayer region, with little of the evidence for interstratification seen in the partially exchanged montmorillonite. On the basis of the single water layer in the interlayer region, Pinnavaia et al.[4] proposed a $[Cu(H_2O)_4]^{2+}$ solvate in the fully exchanged clay, identical with the solvate proposed in this work for $Cu^{2+}$ in partially exchanged montmorillonite. The similar ESR parameters of the two species support the view that the $Cu^{2+}$ solvates in both fully exchanged and partially exchanged montmorillonite are essentially the same, under air-dried conditions, and occupy interlayers containing a single molecular layer of water.

**$Cu^{2+}$ Species C.** It is well established that on dehydration, the exchangeable cations, if possible, enter hexagonal cavities in the silicate lattice.[1] The ESR parameters and ESEM data for species C are consistent with such behavior.

The hexagonal cavities open into the interlayer region though hexagonal ports in the surface of the silicate lattice. The cavities extend into the lattice perpendicular to the lattice layer; see Figure 1. The major axis of symmetry of species C, determined from ESR measurements on oriented films, is also perpendicular to the silicate layers, as would be expected if $Cu^{2+}$ is inside the hexagonal cavity such that its symmetry axes are defined by those of the cavity itself.

ESEM data have been interpreted in terms of coordination to only two deuterium nuclei, implying that the $Cu^{2+}$ carries only one water molecule into the cavity with it. Coordination would therefore be to the lattice OH (undeuterated) and a single $D_2O$ molecule in an axial position. Lattice oxygen atoms, from the tetrahedral silicate layer, would coordinate in equatorial sites. The shift in $g_{\|}$ away from the free spin value on converting species B into species C is consistent with the weak equatorial coordination that would be expected in this chelate.

It was hoped that the $Cu^{2+}$ might be sufficiently close to an $^{27}Al$ nucleus in the octahedral layer of the clay to show coupling, but no modulation from $^{27}Al$ was detected. However, the spin echo signal associated with species C was very weak, and it is possible that weak Al modulation remained undetected. Nevertheless, based on model simulations one can conclude that the $^{27}Al$ nuclei are 0.5 nm or more distant from the $Cu^{2+}$.

The ESR spectrum of species C remained unchanged when the clay was heated to 300 °C under vacuum. It would have been interesting to see whether the single water molecule remained coordinated to $Cu^{2+}$ after heating to this temperature, but samples subjected to such heating exhibited very weak echoes which could not be analyzed for possible modulation.

However, the fact that a change in the characteristics of the echo occurred on heating to 300 °C at least hints that something had changed in the $Cu^{2+}$ environment on extreme dehydration. Supporting this view is the observation that rehydration of the clay resulted in $Cu^{2+}$ returning to its hydrated species A site only if the clay had not been heated above 150 °C. As the dehydration temperature was raised the reversibility of the species A to species C interconversion became less facile. This observation has also been made by McBride and Mortland[23] who proposed that on extreme dehydration exchangeable $Cu^{2+}$ ions in $Cu^{2+}$ montmorillonite migrate irreversibly into the octahedral layer of the clay.

## Conclusion

The combination of X-ray diffraction, ESR, and ESEM measurements have provided a fairly complete picture of the aqueous coordination and location of $Cu^{2+}$-exchanged cations in montmorillonite clay. Three discrete sites are occupied by $Cu^{2+}$ ions, depending on the degree of hydration of the clay. The first, found in fully hydrated montmorillonite, containing several layers of water in the interlayer region, is a freely tumbling $[Cu(H_2O)_6]^{2+}$ solvate similar to that found in a purely aqueous environment. The second, a rotationally restricted $[Cu(H_2O)_4]^{2+}$ solvate, is found in air-dried montmorillonite in which $Cu^{2+}$ ions occupy interlayer regions containing single molecular layers of water. On complete dehydration the $Cu^{2+}$ enters the third site in a hexagonal cavity of the lattice structure. Initially it is associated with one water

(20) Russell, J. D. *Trans. Faraday Soc.* **1965**, *61*, 2284.
(21) Fripiat, J. J. *ACS Symp. Ser.* **1976**, *No. 34*, 261.
(22) Conrad, J. *ACS Symp. Ser.* **1976**, *No. 34*, 85.
(23) McBride, M. B.; Mortland, M. M. *Soil Sci. Soc. Am. Proc.* **1974**, *38*, 408.

molecule in this site. The $Cu^{2+}$ remains in this cavity as the dehydration temperature is raised, becoming irreversibly trapped in the cavity at dehydration temperatures above 150–200 °C.

**Acknowledgment.** This research was supported by the Texas Advanced Technology Research Program and the R.A. Welch Foundation.

**Registry No.** $Cu^{2+}$, 15158-11-9; $Mg^{2+}$, 22537-22-0; montmorillonite, 1318-93-0.

# Theoretical and ESR/ENDOR Single-Crystal Study of an Azaallyl Radical

**Malledi V. V. S. Reddy,[†] Alice Celalyan-Berthier,[†] Michel Geoffroy,*[†] Pierre Y. Morgantini,[‡] Jacques Weber,[‡] and Gerald Bernardinelli[§]**

*Contribution from the Department of Chemistry, University of Geneva, 1211 Geneva 4, Switzerland.* *Received June 12, 1987*

**Abstract:** The room-temperature-stable radical trapped in an X-irradiated single crystal of 2-bromo-5-nitrothiazole has been studied by $^1H$ ENDOR and by ESR. The structure of the undamaged crystal has been determined. The g tensor, the magnetic hyperfine tensors with $^1H$, $^{79}Br$, $^{81}Br$, and the quadrupolar interaction tensors with $^{79}Br$ and $^{81}Br$ have been obtained and their orientations are compared with the bond directions of the original molecule. They lead to the identification of an azaallyl radical R(H)C–N–C(Br)R and give experimental information about the spin delocalization in the C–N–C moiety. The ab initio optimized geometries of $CH_2$–N–$CH_2$ and of $CH_2$–N–CHX (where X = Cl, Br) have been calculated. The theoretical spin densities are obtained together with the calculated magnetic and quadrupolar hyperfine tensors. Experimental results are shown to agree with the theoretical predictions. The possibility of delocalization induced by incorporation of the radical in a thiazolidine ring is also investigated. Allyl and azaallyl structures are compared.

Allyl-type radicals present considerable interest in theoretical and organic chemistry;[1-6] $(C_3H_5)^•$ is indeed the simplest odd-alternate hydrocarbon exhibiting negative spin density on a carbon atom, and allyl derivatives frequently appear as reaction intermediates in heterocyclic chemistry. Curiously, although particular attention has been recently paid to cationic allyl homologues[7-9] containing one or more heteroatoms (e.g., $R_2C$–O–$CH_2^{•+}$, $R_2C$–NH–$CR_2^{•+}$), the simple azaallyl radical, $H_2C$–N–$CH_2$, is considerably less known. It has principally been observed in solution after substitution of the hydrogen atoms by bulky diphenylene groups.[10-11] The results of Grossi et al.,[12] who showed that an azaallylic radical can be created in solution by photolysis of 2-methylthiazoline, together with our recent finding[13] on the trapping of an allyl radical in crystalline nitrothiophene, prompted us to try to generate an azaallylic species in a single crystal of a thiazole derivative. Trapping of this radical in a single-crystal matrix should, indeed, provide the most suitable information for a comparison with quantum chemical calculations.

In the present study, we show that the bromoazaallyl radical **1** can be generated by X-irradiation of a single crystal of bromonitrothiazole **2**. The ESR and ENDOR studies, together with the crystal structure of the undamaged molecule, provide a detailed description of this azaallyl species. Theoretical information is obtained from ab initio calculations performed on the azaallyl radical and some of its derivatives. After optimization of the geometries and calculation of the spin densities, a theoretical estimation of the magnetic and quadrupolar hyperfine interactions

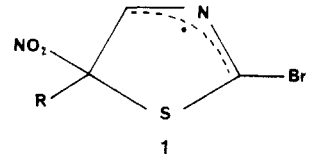


1

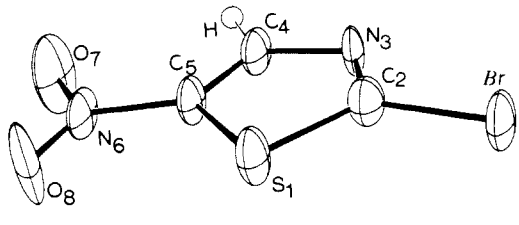


2

**Table I.** Fractional Coordinates and Equivalent Isotropic Temperature Factors, $U_{eq}$ ($Å^2 \times 10^3$)[a]

| | X | Y | Z | $U_{eq}$ |
|---|---|---|---|---|
| Br | 0.5919 (4) | 0.25 | 0.9068 (3) | 43.4 (11) |
| S(1) | 0.7147 (7) | 0.25 | 0.6013 (8) | 41 (3) |
| C(2) | 0.575 (3) | 0.25 | 0.708 (3) | 36 (9) |
| N(3) | 0.4587 (22) | 0.25 | 0.6439 (22) | 33 (8) |
| C(4) | 0.478 (3) | 0.25 | 0.500 (3) | 35 (10) |
| C(5) | 0.607 (3) | 0.25 | 0.4586 (23) | 31 (9) |
| N(6) | 0.658 (3) | 0.25 | 0.3158 (21) | 37 (8) |
| O(7) | 0.5734 (25) | 0.25 | 0.2223 (21) | 77 (11) |
| O(8) | 0.7765 (20) | 0.25 | 0.2985 (23) | 71 (11) |
| H(4) | 0.3945 | 0.25 | 0.4230 | 51 |

[a] Esd's are in parentheses. $U_{eq}$ is the average of the eigenvalues of $U$.

[†] Department of Physical Chemistry.
[‡] Laboratoire de Chimie Théorique Appliquée.
[§] Laboratoire de Cristallographie aux Rayons X.

(1) (a) Heller, C.; Cole, T. *J. Chem. Phys.* **1962**, *37*, 243. (b) Fessenden, R. W.; Schuler, R. H. *Ibid.* **1963**, *39*, 2147.
(2) Takada, T.; Dupuis, M. *J. Am. Chem. Soc.* **1983**, *105*, 1713.
(3) Feller, D.; Davidson, E. R.; Borden, W. T. *J. Am. Chem. Soc.* **1984**, *106*, 2513.
(4) Korth, H. G.; Lomnes, P.; Sustmann, R. *J. Am. Chem. Soc.* **1984**, *106*, 663.
(5) Baird, N. C.; Gupta, R. R.; Taylor, K. F. *J. Am. Chem. Soc.* **1979**, *101*, 4531.
(6) Walton, J. C. *Rev. Chem. Intermed.* **1984**, *5*, 249.
(7) Qin, X. Z.; Williams, F. *J. Phys. Chem.* **1986**, *90*, 2292.
(8) Qin, X. Z.; Snow, L. D.; Williams, F. *J. Am. Chem. Soc.* **1985**, *107*, 3366.
(9) (a) Kispert, L. D.; Pittman, C. U.; Lee Allison, D.; Patterson, T. B.; Gilbert, C. W.; Hains, C. F.; Prather, J. *J. Am. Chem. Soc.* **1972**, *94*, 5979. (b) Lien, M. H.; Hopkinson, A. C. *Can. J. Chem.* **1984**, *62*, 922.
(10) Kuhn, R.; Neugebauer, F. A. *Monatsh. Chem.* **1963**, *94*, 1.
(11) Watanabe, K. *Bull. Chem. Soc. Jpn.* **1975**, *48*, 1732.
(12) Grossi, L.; Lunazzi, L.; Placenti, G. *Tetrahedron Lett.* **1981**, *22*, 251.
(13) Geoffroy, M.; Celalyan-Berthier, A.; Reddy, M. V. V. S.; Bernardinelli, G.; Papadopoulos, M. *J. Chem. Phys.* **1985**, *82*, 4850.

0002-7863/88/1510-2748$01.50/0 